Open charm production in p + p and Pb + Pb collisions at the CERN Large Hadron Collider

2014 J. Phys. G: Nucl. Part. Phys. 41 115101

(http://iopscience.iop.org/0954-3899/41/11/115101)

IOP Publishing Journal of Physics G: Nuclear and Particle Physics
J. Phys. G: Nucl. Part. Phys. **41** (2014) 115101 (23pp) doi:10.1088/0954-3899/41/11/115101

Open charm production in $p+p$ and Pb + Pb collisions at the CERN Large Hadron Collider

V Topor Pop[1], M Gyulassy[2], J Barrette[1], C Gale[1] and M Petrovici[3]

[1] Physics Department, McGill University, Montreal, H3A 2T8, Canada
[2] Physics Department, Columbia University, New York, NY 10027, USA
[3] National Institute for Physics and Nuclear Engineering-Horia Hulubei, R-077125, Bucharest, Romania

E-mail: toporpop@hep.physics.mcgill.ca

Received 30 April 2014, revised 21 July 2014
Accepted for publication 31 July 2014
Published 8 September 2014

Abstract

Effects of strong longitudinal color electric fields, shadowing, and quenching on the production of prompt open charm mesons (D^0, D^+, D^{*+}, D_s^+) in central Pb + Pb collisions at $\sqrt{s_{NN}}$ = 2.76 TeV are investigated within the framework of the HIJING/B$\bar{B}$ v2.0 model. We compute the nuclear modification factor R^D_{PbPb}, and show that the above nuclear effects constitute important dynamical mechanisms in the description of experimental data. The strength of color fields (as characterized by the string tension κ), partonic energy loss and jet quenching process lead to a suppression factor consistent with recent published data. Predictions for beauty mesons are presented. In addition, ratios of strange to non-strange prompt charm mesons in central Pb + Pb and minimum bias (MB) $p + p$ collisions at 2.76 TeV are also discussed. MB $p + p$ collisions which constitute a theoretical baseline in our calculations are studied at centre of mass energies $\sqrt{s}$ = 2.76 TeV and 7 TeV.

Keywords: heavy ion collisions, phenomenological models, phenomenology

(Some figures may appear in colour only in the online journal)

1. Introduction

The phase transition from hadronic to partonic degrees of freedom in ultra-relativistic nuclear collisions is a central focus of experiments at the CERN Large Hadron Collider (LHC) [1–4]. Heavy-flavour quarks are an ideal probe to study early dynamics ($\tau < 1$ fm c^{-1}) in these

nuclear collisions. Several theoretical studies predict a substantial enhancement of open charm production, associated with the formation of a plasma of deconfined parton matter relative to the case of a purely hadronic scenario without plasma formation [5–9]. For reviews of heavy-flavour production in heavy-ion collisions see ref. [10–13]. The study of open charm production allows one to probe the mechanisms of heavy-quark propagation, energy loss and hadronization in the hot dense medium formed in high-energy nucleus–nucleus collisions [12–16]. Heavy quarks are key observables in the study of thermalization of the initially created hot nuclear matter [17, 18].

Owing to their large mass, heavy quarks are produced predominantly in the initial phase of the collision via gluonic fusion processes [19] and therefore probe the complete space–time evolution of the quark gluon plasma (QGP) matter. Their production rates are expected to be well described by perturbative quantum cromodynamics (pQCD) at fixed order plus next to-leading logarithms (FONLL) [20–22]. Measurements at Relativistic Heavy Ion Collider (RHIC) energies [23–26] have shown that the gluon fusion process could also dominate in heavy-ion collisions and that thermal processes might contribute later at low transverse momentum [27].

The production and propagation of hard probes in nucleus–nucleus ($A + A$) collisions can be quantified by the nuclear modification factor (NMF)

$$R_{\mathrm{AA}}(p_{\mathrm{T}}) = \frac{\left(1/N_{\mathrm{evt}}^{\mathrm{AA}}\right)\mathrm{d}^2 N_{\mathrm{AA}}/\mathrm{d}^2 p_{\mathrm{T}}\,\mathrm{d}y}{N_{\mathrm{coll}}\left(1/N_{\mathrm{evt}}^{\mathrm{pp}}\right)\mathrm{d}^2 N_{\mathrm{pp}}/\mathrm{d}^2 p_{\mathrm{T}}\,\mathrm{d}y}, \tag{1}$$

where, N_{evt} is the number of events and N_{coll} is the average number of binary nucleon–nucleon (NN) collisions, and $\mathrm{d}^2 N/\mathrm{d}^2 p_{\mathrm{T}}\,\mathrm{d}y$ stand for the transverse momentum (p_{T}) and rapidity (y) differential yield of an observable measured in $A + A$ or proton–proton ($p + p$) collisions. A value $R_{\mathrm{AA}}(p_{\mathrm{T}}) \neq 1$ would indicate contributions from initial and final-state effects. These observables provide stringent constraints on theoretical predictions, in particular jet quenching in $A + A$ collisions at RHIC and at LHC energies.

One of the most exciting discoveries at RHIC, was that heavy quark is suppressed by an amount similar to that of light quarks, for transverse momentum $p_{\mathrm{T}} > 5$ GeV c^{-1} [28] (the open charm RHIC puzzle). This result was a surprise; it appears to disfavour the energy loss explanation of suppression [29, 30] based on the fact that heavy quarks should radiate much less than light quarks or gluons. In addition, the dead-cone effect [31] and other mechanisms [32, 33] are expected to introduce a mass-dependence in the coupling of hard partons with the medium constituents. A possible solution to this puzzle [28, 34] is based on the assumption that in the standard model, the Higgs Boson, which gives mass to the electro-weak vector bosons, does not necessarily gives mass to fermions and it can not be excluded that in a QCD colored world, all six quarks are nearly massless.

The non-perturbative particle creation mechanisms in strong external fields has a wide range of application not only in original $\mathrm{e}^+\mathrm{e}^-$ pair creation on quantum electrodynamics (QED) problems [35], but also for pair creation (fermions and bosons) in strong non-Abelian electromagnetic fields [36–47]. In a high-energy heavy-ion collision, strong color fields are expected to be produced between the partons of the projectile and target. Theoretical descriptions of particle production in high energy $p + p$ and $A + A$ collisions are based on the introduction of chromoelectric flux tube (*strings*) models [48, 49]. The string breaking picture [48] is a good example of how to convert the kinetic energy of a collision into field energy. Therefore, the Schwinger mechanism is assumed to be an important mechanism for hadronic production. For a uniform chromoelectric flux tube with field (E) the probability to create a pair of quarks with mass (m), effective charge ($e_{\mathrm{eff}} = \mathrm{e}/3$), and transverse momentum

(p_T) per unit time and per unit volume is given by [50]

$$P(p_T)\mathrm{d}^2p_T = -\frac{|e_{\mathrm{eff}}E|}{4\pi^3}\ln\left\{1-\exp\left[-\frac{\pi\left(m^2+p_T^2\right)}{|e_{\mathrm{eff}}E|}\right]\right\}\mathrm{d}^2p_T. \quad (2)$$

The integrated probability (P_m) reproduces the classical Schwinger results [35], derived in spinor QED for e^+e^- production rate, when the leading term in equation (2) is taken into account, i.e.:

$$P_m = \frac{\left(e_{\mathrm{eff}}E\right)^2}{4\pi^3}\sum_{n=1}^{\infty}\frac{1}{n^2}\exp\left(-\frac{\pi\, m^2 n}{|e_{\mathrm{eff}}E|}\right). \quad (3)$$

In a string fragmentation phenomenology, it has been proposed that the observed strong enhancement of strange particle production in nuclear collisions could be naturally explained via strong longitudinal color field effects [37]. Recently, an extension of color glass condensate (CGC) theory has proposed a more detailed dynamical 'GLASMA' model [51–53] of color ropes. In the string models, strong longitudinal fields (flux tubes, effective strings) decay into new ones by quark anti-quark ($q\bar{q}$) or diquark anti-diquark (qq–$\overline{qq}$) pair production and subsequently hadronize to produce the observed hadrons. Due to confinement, the color of these strings is restricted to a small area in transverse space [41]. With increasing energy of the colliding particles, the number of strings grows and they start to overlap, forming clusters. This can introduce a possible dependence of particle production on the energy density [54].

Heavy Ion Jet Interacting (HIJING) type models such as HIJING1.0 [49], HIJING2.0 [55, 56] and HIJING/B$\bar{\mathrm{B}}$ v2.0 [57–65], have been developed to study hadron productions in $p + p$, $p + A$ and $A + A$ collisions. These models are based on a two-component geometrical model of mini-jet production and soft interactions and has incorporated nuclear effects such as *shadowing* (nuclear modification of the parton distribution functions (PDFs)) and *jet quenching*, via final state jet medium interactions. In the HIJING/B$\bar{\mathrm{B}}$ v2.0 model [59, 61] we introduced new dynamical effects associated with long range coherent fields (i.e., strong longitudinal color fields, SCF), including baryon junctions and loops [58, 66]. At RHIC energies we have shown [57–59] that the dynamics of strangeness production deviates considerably from calculations based on Schwinger-like estimates for homogeneous and constant color fields [35], and points to the possible contribution of fluctuations of transient strong color fields (SCF). These fields are similar to those which could appear in a *glasma* [52] at the initial stage of the collisions. In a scenario with QGP phase transitions the typical field strength of SCF at RHIC energies was estimated to be about 5–12 GeV fm^{-1} [67].

The tunneling process mechanism of heavy Q$\bar{\mathrm{Q}}$ pair production has been revisited [68] and pair production in time-dependent electric fields have been studied [69]. It is concluded that particles with large momentum are likely to have been created earlier than particles with small momentum, and in addition, during a very short period $\Delta\tau$ ($\Delta\tau \approx 10t_Q$, where the Compton time $t_Q = 1/m_Q$) the standard Schwinger formula (i.e. with a constant electric field), strongly underestimates the particle number density.

In a previous paper [60] effects of strong longitudinal color electric fields (SCF) on the open charm production in nucleus–nucleus ($A + A$) collisions at RHIC energies were investigated within the framework of the HIJING/B$\bar{\mathrm{B}}$ v2.0 model [57–59]. It was shown that a three fold increase of the effective string tension results in a sizeable enhancement (≈60–70%) of the total open charm production cross-sections ($\sigma_{c\,\bar{c}}^{\mathrm{NN}}$) in comparison with the results obtained without SCF effects. At design LHC energy ($\sqrt{s} = 14$ TeV) the HIJING/B$\bar{\mathrm{B}}$ v2.0 model predicts an increase in $p + p$ collisions of $\sigma_{c\,\bar{c}}^{\mathrm{NN}}$ by approximately an order of

magnitude [60]. Moreover, in this work we offer an alternative explanation of the open charm RHIC puzzle since the calculated NMF of D^0 mesons shows at moderate transverse momentum (p_T) a suppression consistent with RHIC data [23–26]. String fusion and percolation effects on heavy flavour production have also been discussed in refs. [70, 71] at RHIC and LHC energies. The production pattern for heavy quarks in both of these non-perturbative approaches becomes similar to that of the light quarks via the Schwinger mechanism [35] and result on an expected enhancement of heavy quark pairs $Q\bar{Q}$.

Recently, the total open charm cross-sections were reported in $p + p$ collisions at $\sqrt{s} = 2.76$ and $\sqrt{s} = 7$ TeV by ALICE [72–74] , ATLAS [75–77] and LHCb [78] Collaborations. Measurements of open-heavy flavour p_{T} differential production cross-sections ($\sigma_{\mathrm{inel}} \mathrm{d}^2 N_{\mathrm{AA}} / \mathrm{d}^2 p_{\mathrm{T}} \mathrm{d}y$) in Pb + Pb Collisions at a center of mass energy per nucleon pair $\sqrt{s_{\mathrm{NN}}} = 2.76$ TeV have also been published by the ALICE Collaboration [15, 16, 79–82].

In $p + p$ collisions at $\sqrt{s} = 7$ TeV the p_{T}-differential production cross-sections of prompt charmed mesons (D^0, D^+, D^{*+}, D_s^+) at mid-rapidity ($|y| < 0.5$) are compatible with the upper limit of the FONLL predictions [83], leaving room for possible new dynamical mechanisms. Note that, the models with different parametrization of un-integrated gluon distributions (UGDF) significantly underpredict the experimental data [83]. In contrast models implementing a general-mass variable-flavour-number scheme (GM-VFNS) predict rates higher than the observed data [84].

RHIC results show that heavy quark lose energy in the medium, but a possible quark-mass hierarchy predicted in ref. [32] has not been established, i.e., a smaller suppression expected when going from the mostly gluon-originated light flavour hadrons (e.g., pions) to D and B mesons [79]. At LHC energies, prompt D mesons present a similar suppression as charged particles and this observation is challenging for most theoretical and phenomenological analysis [15, 16]. The model calculations for NMFs of prompt charmed mesons in Pb + Pb collisions at $\sqrt{s_{\mathrm{NN}}} = 2.76$ TeV indicate a reasonable agreement with data [85–93] but only for moderate and high transverse momentum (p_{T}), i.e. $p_{\mathrm{T}} > 5$ GeV c^{-1}, where the suppression is a factor of 2.5–4 in comparison with binary scaling [79]. However, the description at low transverse momentum ($p_{\mathrm{T}} \leqslant 4$ GeV c^{-1}) is more challenging for the currently available theoretical model calculations. The expected p + Pb collisions data will provide new valuable information on possible initial-state effects in the low-momentum region.

The HIJING/B$\bar{\mathrm{B}}$ v2.0 model has successfully described the global observables and identified particle (ID) data, including (multi)strange particles production in p+p [61, 64] p + Pb [63, 65] and Pb + Pb collisions [62] at RHIC and LHC energies. In this paper we extend our study to prompt open charm mesons production (D^0, D^+, D^{*+}, D_s^+) as measurements have been recently published [72–74]. The setup and input parameters used here are taken from previous works (see refs. [62, 64, 65]). We explore dynamical effects associated with long range coherent fields (i.e. strong color fields, SCF), including baryon junctions and loops, with emphasis on the novel open charm observables measured at LHC energies in p+p collisions at $\sqrt{s} = 2.76$ and $\sqrt{s} = 7$ TeV. The nuclear final state effects (jet quenching) and initial state effects (shadowing) are discussed for the NMFs $R_{\mathrm{AA}}(p_{\mathrm{T}})$ measured in Pb + Pb collisions at $\sqrt{s_{\mathrm{NN}}} = 2.76$ TeV [79–82]. In addition, in order to better identify initial state effects, predictions for NMF $R_{\mathrm{pA}}(p_{\mathrm{T}})$ in p + Pb collisions at $\sqrt{s_{\mathrm{NN}}} = 5.02$ TeV are also presented.

2. Outline of HIJING/B$\bar{\text{B}}$ v2.0 model. setup and input

2.1. Strong color field. string tension

In this paper we present the results of calculations for different observables measured in $p + p$, p + Pb and Pb + Pb collisions at LHC energies. Therefore, we consider it useful to the reader to include a summary of the main input parameters which have been determined in refs. [62, 64, 65] and that are used in the present analysis. This is the subject of section 2 where we describe the basic phenomenology embedded in the HIJING/B$\bar{\text{B}}$ v2.0 model.

Based on the assumption that the Higgs Boson, which gives mass to the electro-weak vector bosons, does not necessarily gives mass to fermions and that in a QCD colored world, all six quarks are nearly massless [34], we investigate if the Schwinger mechanism could play a role in the non-perturbative soft production of heavy quarks ($Q = c$, or b), within the framework of the HIJING/B$\bar{\text{B}}$ model. For a uniform chromoelectric flux tube with field (E), for a heavy quark pair ($Q\bar{Q}$) the production rate per unit volume is given by [37, 68, 69]

$$\Gamma = \frac{\kappa^2}{4\pi^3} \exp\left(-\frac{\pi\, m_Q^2}{\kappa}\right), \tag{4}$$

Note that Γ is given by the first term in the series of integrated probability P_m (equation (3)). For $Q = c$ (charm) or $Q = b$ (bottom), $m_Q = 1.27$, or 4.16 GeV (with $\pm 1\%$ uncertainty [94]), and $\kappa = |e_{\text{eff}} E|$ is the effective string tension. For a color rope, if the *effective* string tension value (κ) increases from vacuum value $\kappa = \kappa_0 = 1.0\,\text{GeV fm}^{-1}$ to an in medium value $\kappa = 3.0\,\text{GeV fm}^{-1}$, the pair production rate per unit volume for charm pairs would increase from $\approx 1.4 \times 10^{-12}$ to $\approx 3.5 \times 10^{-4}$ fm^{-4}. This can lead to a net soft tunneling production comparable to the initial hard FONLL pQCD prediction. In the HIJING/B$\bar{\text{B}}$ model (which is a two component model) the string/rope fragmentation is the only soft source of multiparticle production and multiple minijets provide a semi-hard additional source that is computable within collinear factorized standard pQCD with initial and final radiation (DGLAP evolution [95]).

A measurable rate for spontaneous pair production requires strong chromoelectric fields, such that $\kappa/m_Q^2 > 1$ some of the time. Introducing a strong longitudinal electric field within string models, result in a highly suppressed production rate of heavy $Q\bar{Q}$ pair ($\gamma_{Q\bar{Q}}$) related to light quark pairs ($q\bar{q}$). From equation (4) one obtain [68] the suppression factor $\gamma_{Q\bar{Q}}$

$$\gamma_{Q\bar{Q}} = \frac{\Gamma_{Q\bar{Q}}}{\Gamma_{q\bar{q}}} = \exp\left(-\frac{\pi\left(m_Q^2 - m_q^2\right)}{\kappa}\right), \tag{5}$$

The suppression factors are calculated for $Q = qq$ (diquark), $Q = s$ (strange), $Q = c$ (charm), or $Q = b$ (bottom) ($q = u,\ d$ stand for light quarks).

The current quark masses are $m_{qq} = 0.45$ GeV [96], $m_s = 0.12$ GeV, $m_c = 1.27$ GeV, and $m_b = 4.16$ GeV [97]. The constituent quark masses of light non-strange quarks are $M_{u,d} = 0.23$ GeV, of the strange quark is $M_s = 0.35$ GeV [98], and of the diquark is $M_{qq} = 0.55 \pm 0.05$ GeV [96]. In our calculations, we use $M_{qq}^{\text{eff}} = 0.5$ GeV, $M_s^{\text{eff}} = 0.28$ GeV, $M_c^{\text{eff}} = 1.27$ GeV. Therefore, for the vacuum string tension value $\kappa_0 = 1\,\text{GeV fm}^{-1}$, the above formula from equation (5) results [64] in a suppression of heavier quark production according to $u : d : qq : s : c \approx 1 : 1 : 0.02 : 0.3 : 10^{-11}$. For a color rope, on the other hand, if the effective string tension value κ increases to $\kappa = f_\kappa \kappa_0$ (with $f_\kappa > 1$) the value of $\gamma_{Q\bar{Q}}$ increases. Equivalently, a similar increase of $\gamma_{Q\bar{Q}}$ could be obtained by a decrease of quark masses from

m_Q to $m_Q/\sqrt{f_\kappa}$. We have shown that this dynamical mechanism improves considerably the description of the strange meson/hyperon data at the Tevatron and at LHC energies [61].

At ultra-high energy, $A + A$ collisions can also be described as two colliding sheets of CGC. In the framework of this model it was shown that in the early stage of collisions a strong longitudinal color-electric field is created [51]. Saturation physics is based on the observation that small-x hadronic and nuclear wave functions, and, thus the scattering cross-sections as well, are described by the same internal momentum scale known as the saturation scale, $Q_{\rm sat}$. In $p + p$ collisions at LHC energies the saturation scale is proportional to the charged particle density at mid-rapidity, $Q^2_{\rm sat,\,p}(s) \propto ({\rm d}N_{\rm ch}/{\rm d}\eta)_{\eta=0}$. An analysis of $p + p$ data up to $\sqrt{s} = 7$ TeV has shown that, with the k_T factorized gluon fusion approximation [99], the growth of the charged particle density at mid-rapidity can be accounted for [100] if the saturation scale grows with centre of mass (c.m.) energy ($\sqrt{s}$) as:

$$Q^2_{\rm sat,\,p}(s) = Q^2_{0\rm p}(s/s_0)^{\lambda_{\rm CGC}}, \tag{6}$$

with $\lambda_{\rm CGC} \approx 0.11$. It has been argued that, in nucleus–nucleus collisions, the saturation scale also grows with atomic number. A natural option is to assume that $Q^2_{\rm sat,\,A}$ is proportional to the number of participants in the collisions, i.e., as $Q^2_{\rm sat,\,A} \propto Q^2_{\rm sat,\,p}(s)A^{1/3}$ [53].

In the CGC model, it has been proposed that the gluonic partons produce flux tubes with an original width of transverse size, of the order of $1/Q_{\rm sat,A}$ [101, 102]. These flux tubes persist during the evolution of QGP. In the Lund hadronization model [48, 49], the large number of particles produced in heavy ion collisions are reproduced using string fragmentation. When a pair of QCD charge and anti-charge are pulled apart, a flux tube of fields develops between the pair. These flux tubes are extended and nonlinear objects, and for modelling are approximated by a thin string. They have been observed in Latice QCD [41]. The flux tubes utilized to simulate $A + A$ collisions may have a string tension almost one order of magnitude larger than the fundamental string tension linking a mesonic quark-antiquark pair [36, 41].

The initial energy densities in the collisions ($\epsilon_{\rm ini}$) are computed from the square of the field components [41]. Within our phenomenology $\epsilon_{\rm ini}$ is proportional to the mean field values $\langle E^2\rangle$, and using the relation $\kappa = e_{\rm eff}E$, means $\epsilon_{\rm ini} \propto \kappa^2$. Using the Bjorken relation the $\epsilon_{\rm ini}$ is proportional with charged particle density at mid-rapidity , and thus $\kappa^2 \propto ({\rm d}N_{\rm ch}/{\rm d}\eta)_{\eta=0}$. A similarity with the phenomenology embedded in the CGC model is obvious, and we obtain $\kappa \propto Q_{\rm sat,p}$ as discussed in [61]. In [61], to describe the energy dependence of the charged particle density at mid-rapidity in $p + p$ collisions up to the LHC energies, we use a power law dependence

$$\kappa(s) = \kappa_0\,(s/s_0)^{0.06}\ \ {\rm GeV\ fm^{-1}}, \tag{7}$$

consistent (within the fit errors) of that deduced in CGC model [100].

We have shown in [64] that combined effects of hard and soft sources of multiparticle production as embedded in the HIJNG/B$\bar{\rm B}$ v2.0 model can reproduce the charged particle density at mid-rapidity and the identified particle spectra (including (multi)strange particles) in $p + p$ collisions in the range $0.02 < \sqrt{s} < 7$ TeV, by an energy dependent string tension $\kappa(s)$, with a somewhat reduced power law :

$$\kappa(s) = \kappa_0\,(s/s_0)^{0.04}\ \ {\rm GeV\ fm^{-1}}. \tag{8}$$

This new parameterization (i.e., equation (8)) does not affect significantly the entropy embedded in the model and the charged particle densities at mid-rapidity are also well described (see [64]). equation (8) leads to an increasing value for the mean string tension from

$\kappa = 1.5\,\mathrm{GeV\,fm^{-1}}$ at $\sqrt{s} = 0.2\,\mathrm{TeV}$ (top RHIC energy) to $\kappa = 2.0\,\mathrm{GeV\,fm^{-1}}$ at $\sqrt{s} = 7\,\mathrm{TeV}$. The sensitivity of the calculations to string tension values (κ) for different observables have been studied in previous papers [58–62, 64].

This constitute the only modification of the model parameters discussed in our previous paper [64]. Our phenomenological parameterization equation (8), is strongly supported by data on charged particle densities at mid-rapidity ($\sqrt{(\mathrm{d}N_{\mathrm{ch}}/\mathrm{d}\eta)_{\eta=0}}$). Within the statistical errors the energy dependence of $\sqrt{(\mathrm{d}N_{\mathrm{ch}}/\mathrm{d}\eta)_{\eta=0}}$ data is consistent with a power law proportional to $s^{0.05}$ for inelastic $p + p$ interactions and to $s^{0.055}$ for non-single diffractive events [118, 116].

In addition, in $A + A$ collisions the effective string tension value could also increase due to in-medium effects [62], or possible dependence on number of participants. This increase is also quantified in our phenomenology by an analogy with CGC model. We consider for the mean value of the string tension an energy and mass dependence, $\kappa(s, A) \propto Q_{\mathrm{sat,A}}(s, A) \propto Q_{\mathrm{sat,p}}(s)A^{1/6}$. Therefore, for $A + A$ collisions we use in the present analysis, a power law dependence $\kappa = \kappa(s, A)$

$$\kappa(s, A)_{\mathrm{LHC}} = \kappa(s)A^{0.167} = \kappa_0\,(s/s_0)^{0.04}A^{0.167}\ \ \mathrm{GeV\,fm^{-1}}. \tag{9}$$

Equation 9 leads to $\kappa(s, A)_{\mathrm{LHC}} \approx 5\,\mathrm{GeV\,fm^{-1}}$, in Pb +Pb collisions at c.m. energy per nucleon $\sqrt{s_{\mathrm{NN}}} = 2.76\,\mathrm{TeV}$. First heavy-ion data at the LHC, i.e., charged particle density and NMF R_{PbPb} are only slightly different (see section 3.2, figure 2) than those calculated in ref. [62] where a higher value of κ, $\kappa(s, A)_{\mathrm{LHC}} = \kappa_0\,(s/s_0)^{0.06}A^{0.167} \approx 6\,\mathrm{GeV\,fm^{-1}}$ was used. The reason for this small effect is that the suppression factors $\gamma_{Q\bar{Q}}$, approach unity in Pb + Pb collisions at $\sqrt{s_{\mathrm{NN}}} = 2.76\,\mathrm{TeV}$, for the string tension values $\kappa \geqslant 5\,\mathrm{GeV\,fm^{-1}}$.

The mean values of the string tension $\kappa(s)$ for $p + p$ collisions (equation (8)) and $\kappa(s, A)$ for $A + A$ collisions (equation (9)) are used in the present calculations. These lead to a related increase of the various suppression factors, as well as an enhancement of the intrinsic (primordial) transverse momentum k_T. These include: (i) the ratio of production rates of diquark-quark to quark pairs (diquark-quark suppression factor), $\gamma_{qq} = \Gamma(qq\overline{qq})/\Gamma(q\bar{q})$; (ii) the ratio of production rates of strange to non-strange quark pairs (strangeness suppression factor), $\gamma_s = \Gamma(s\bar{s})/\Gamma(q\bar{q})$; (iii) the extra suppression associated with a diquark containing a strange quark compared to the normal suppression of strange quark (γ_s), $\gamma_{us} = (\Gamma(\mathrm{us\overline{us}})/\Gamma(\mathrm{ud\overline{ud}}))/(\gamma_s)$;(iv) the suppression of spin 1 diquarks relative to spin 0 ones (in addition to the factor of 3 enhancement of the former based on counting the number of spin states), γ_{10}; and (v) the (anti)quark ($\sigma_q'' = \sqrt{\kappa/\kappa_0}\cdot\sigma_q$) and (anti)diquark ($\sigma_{qq}'' = \sqrt{\kappa/\kappa_0}\cdot f\cdot\sigma_{qq}$) Gaussian width of primordial (intrinsic) transverse momentum k_T. In the above formulae for σ_q'' and σ_{qq}'' we use $\sigma_q = \sigma_{qq} = 0.350\,\mathrm{GeV\,c^{-1}}$ as default value (in absence of SCF effects) for Gaussian width of the quark (diquark) intrinsic transverse momentum distribution.

Moreover, to better describe the baryon/meson anomaly seen in data at RHIC and LHC energies, a specific implementation of JJ̄ loops, had to be introduced (for details see refs. [62, 64]). The absolute yield of charged particles, $\mathrm{d}N_{\mathrm{ch}}/\mathrm{d}\eta$ is also sensitive to the low $p_{\mathrm{T}} < 2\,\mathrm{GeV\,c^{-1}}$ non-perturbative hadronization dynamics that is performed via LUND [105] string excitation and hadronization mechanisms. Multiple low $p_{\mathrm{T}} < 2\,\mathrm{GeV\,c^{-1}}$ transverse momentum color exchanges excite the incident baryons into longitudinal strings that fragment due to color neutralization into an array of physical hadron resonance states. The conventional hard pQCD mechanisms are calculated in HIJING/BB̄ v2.0 via the hard processes encoded in PYTHIA/JETSET event generators [106, 107]. The advantage of HIJING/BB̄ v2.0 over PYTHIA is the ability to include novel SCF color rope effects that arise from longitudinal

color fields, while amplified by the random walk in color space of the high x valence partons in $A + A$ collisions. This random walk could induce a very broad fluctuation spectrum of the effective string tension.

In the present work we will study only the effect of a larger effective value $\kappa > 1$ GeV fm^{-1} on the production of prompt charmed mesons (D^0, D^+, D^{*+}, D_s^+) measured in Pb + Pb and $p + p$ collisions at LHC energies. The model is based on the time-independent strength of color field while in reality the production of $Q\bar{Q}$ pairs is a far-from-equilibrium, time and space dependent complex phenomenon. Therefore, we can not investigate in details possible fluctuations which could appear due to these more complex dependences.

2.2. Nuclear shadowing and jet quenching

As mentioned above, in HIJING the string/rope fragmentation is not the only *soft source* of multiparticle production and multiple minijets provide a semi-hard additional source that is computable within collinear factorized standard pQCD with initial and final radiation (DGLAP evolution [95]). Within the HIJING model, one assumes that NN collisions at high energy can be divided into *soft* and *hard* processes with at least one pair of jet with transverse momentum, $p_T > p_0$. A cut-off (or saturation) scale p_0 in the final jet production has to be introduced below which the high density of initial interactions leads to a non-perturbative mechanism which in the HIJING framework is characterized by a finite soft parton cross-section σ_{soft}. The inclusive jet cross-section σ_{jet} at leading order (LO) [108] is

$$\sigma_{jet} = \int_{p_0^2}^{s/4} dp_T^2 dy_1 dy_2 \frac{1}{2} \frac{d\sigma_{jet}}{dp_T^2 dy_1 dy_2}, \tag{10}$$

where

$$\frac{d\sigma_{jet}}{dp_T^2 dy_1 dy_2} = K \sum_{a,b} x_1 f_a\left(x_1, p_T^2\right) x_2 f_b\left(x_2, p_T^2\right) \frac{d\sigma^{ab}\left(\hat{s}, \hat{t}, \hat{u}\right)}{d\hat{t}} \tag{11}$$

depends on the parton–parton cross-section σ^{ab} and PDFs, $f(x, p_T^2)$. The summation runs over all parton species; y_1 and y_2 are the rapidities of the scattered partons; x_1 and x_2 are the light-cone momentum fractions carried by the initial partons. The multiplicative K factor ($K \approx 1.5$–2) account for the next-to-leading order (NLO) corrections to the LO jet cross-section [109, 110]. In the default HIJING model [49, 111], the Duke–Owens parameterization [112] for PDFs of nucleons is used. With the Duke–Owens parameterization for PDFs, an energy independent cut-off scale $p_0 = 2$ GeV c^{-1} and a constant soft parton cross-section $\sigma_{soft} = 57$ mb are sufficient to reproduce the experimental data on total and inelastic cross-sections and the hadron central rapidity density in $p + p(\bar{p})$ collisions [49, 111].

The largest uncertainty in mini-jet cross-sections is the strong dependence on the minimum transverse momentum scale cut-off, p_0. In this paper the results for $p + p$ collisions are obtained using the same set of parameters for hard scatterings as in the default HIJING model [111]. Using a constant momentum cut-off $p_0 = 2$ GeV c^{-1} in central $A + A$ collisions, the total number of minijets per unit transverse area for independent multiple jet production, could exceed the limit [55, 56]

$$\frac{T_{AA}(b)\sigma_{jet}}{\pi R_A^2} \leqslant \frac{p_0^2}{\pi}, \tag{12}$$

where $T_{AA}(b)$ is the overlap function of $A + A$ collisions and π/p_0^2 is the intrinsic transverse size of a minijet with transverse momentum p_0. Therefore, an increased value of p_0 with c.m.

energy per nucleon $\sqrt{s_{\rm NN}}$ is required by the experimental data indicating that the *coherent interaction* becomes important. Moreover, we have to consider an energy and nuclear size dependent cut-off $p_0(s, A)$, in order to ensure the applicability of the two-component model for $A + A$ collisions. It was shown [62] that the pseudorapidity distribution of charged particles in central nucleus–nucleus collisions at RHIC and LHC energies can be well described if we consider a scaling law of the type $CA^{\alpha}\sqrt{s}^{\beta}$

$$p_0(s, A) = 0.416\, A^{0.128}\ \sqrt{s}^{\ 0.191}\ \text{GeV}\ c^{-1} \tag{13}$$

A similar dependence was used in pQCD + saturation model to predict global observables at LHC energies [113]. The main difference is the value of the proportionality constant ($C_{\rm HIJ} = 0.416$ versus $C_{\rm esk} = 0.208$). The value $C_{\rm esk} = 0.208$ used in [113, 114] results in an overestimate of the charged particle density by a factor of approximately two at LHC energies. These effective values are not expected to be valid for peripheral $A + A$ or for $p + p$ collisions.

The above limit for incoherent mini-jet production should in fact also depend on impact-parameter [115]. Such dependence is not included in the present calculations. Instead, in the HIJING model an impact-parameter dependence of the gluon shadowing is considered in the parameterization of the parton shadowing factor $S_{a/A}$ (see below). Due to shadowing effects the observed A-exponent ($\alpha = 0.128$) in equation (13) is somewhat less than the number expected in the saturated scaling limit ($p_0(s, A) \sim A^{1/6}$) [114].

One of the main uncertainty in calculating charged particle multiplicity density in Pb + Pb collisions is the nuclear modification of PDFs, especially gluon distributions at small x. In HIJING-type models, one assumes that the parton distribution in a nucleus (with atomic number A and charge number Z), $f_{a/A}(x, Q^2)$, are factorizable into parton distributions of nucleons ($f_{\rm a/N}$) and the parton(a) shadowing factor ($S_{a/A}$),

$$f_{a/A}\left(x, Q^2\right) = S_{a/A}\left(x, Q^2\right) A f_{\rm a/N}\left(x, Q^2\right). \tag{14}$$

We assume that the shadowing effect for gluons and quarks is the same, and neglect also the QCD evolution (Q^2 dependence of the shadowing effect). At this stage, the experimental data unfortunately can not fully determine the A dependence of the shadowing effect. We follow the A dependence as proposed in ref. [49] and use the following parametrization:

$$\begin{aligned} S_{a/A}(x) \ &\equiv\ \frac{f_{a/A}(x)}{A f_{\rm a/N}(x)} \\ &=\ 1 + 1.19\log^{1/6}\!A\left[x^3 - 1.2x^2 + 0.21x\right] \\ &\quad - s_{\rm a}\left(A^{1/3} - 1\right)\left[1 - \frac{10.8}{\log(A+1)}\sqrt{x}\right]\mathrm{e}^{-x^2/0.01}, \end{aligned} \tag{15}$$

$$s_{\rm a} = 0.1. \tag{16}$$

The term proportional to $s_{\rm a}$ in equation (15) determines the shadowing for $x < x_0 = 0.1$, and has the most important nuclear dependence, while the rest gives the overall nuclear effect on the structure function in $x > x_0$ with some very slow A dependence. This parametrization can fit the overall nuclear effect on the quark structure function in the small and medium x region [49]. Because the remaining term of equation (15) has a very slow A dependence, we consider only the impact parameter dependence of $s_{\rm a}$. In fact most of the jet production occurs in the small x region where shadowing is important:

$$s_{\rm a}(b) = s_{\rm a}\frac{5}{3}\Big(1 - b^2/R_{\rm A}^2\Big). \tag{17}$$

In the above equation $R_{\rm A}$ is the radius of the nucleus, and the factor $s_{\rm a}$ is taken the same for quark and for gluon $s_a = s_Q = s_g = 0.1$.

The LHC data indicate that such quark (gluon) shadowing is required to fit the centrality dependence of the central charged particle multiplicity density in Pb + Pb collisions [62]. This constraint on quark (gluon) shadowing is indirect and model dependent. Therefore, it will be important to study quark(gluon) shadowing in $p + A$ collisions at the LHC. In contrast, in HIJING2.0 [55, 56], a different A parametrization ($(A^{1/3} - 1)^{0.6}$) and much stronger impact parameter dependence of the gluon (s_g= 0.22–0.23) and quark ($s_{\rm q} = 0.1$) shadowing factor is used in order to fit the LHC data. Because of this stronger gluon shadowing the jet quenching effect is neglected [55]. Note, all HIJING-type models assume a scale-independent form of shadowing parametrization (fixed Q^2). This approximation could break down at very large scale due to the dominance of gluon emission dictated by the DGLAP [95] evolution equation. The default HIJING1.0 parametrization of the fixed $Q_0^2 = 2\,{\rm GeV}^2$ shadowing function [49] leads to a substantial reduction at the LHC of the global multiplicity in p + Pb and Pb + Pb collisions. It is important to emphasize that the *no shadowing* results are substantially reduced in HIJING/B$\bar{\rm B}$ 2.0 [62, 63, 65], relative to the *no shadowing* predictions within HIJING/1.0 from ref. [49], because both the default minijet cut-off $p_0 = 2\,{\rm GeV\,c^{-1}}$ and the default vacuum string tension $\kappa_0 = 1\,{\rm GeV\,fm^{-1}}$ (used in HIJING1.0) are generalized to vary monotonically with c.m. energy $\sqrt{s}$ and atomic number, A.

As discussed above, systematics of $p + p$ and Pb+Pb multiparticle production from RHIC to the LHC are used here to fix the energy ($\sqrt{s}$) and the A dependence of the cut-off parameter $p_0(s, A) = 0.416\ \sqrt{s}^{0.191}\ A^{0.128}\,{\rm GeV\,c^{-1}}$ and the mean value of the effective string tension $\kappa(s, A) = \kappa_0\ (s/s_0)^{0.04}\ A^{0.167}\,{\rm GeV\,fm^{-1}}$ in $A + A$ collisions [64]. For p + Pb collisions at $\sqrt{s_{\rm NN}} = 5.02$ TeV, the above formulae lead to $p_0 = 3.1\,{\rm GeV\,c^{-1}}$ (calculated as a mean value of $p_0^{\rm PbPb} = 4.2\,{\rm GeV\,c^{-1}}$ and $p_0^{\rm pp} = 2\,{\rm GeV\,c^{-1}}$). The measurement of initial energy density produced in p + Pb collisions would help us to determine better the effective value of the string tension κ in$p$ + Pb collisions. Therefore, in the present calculations we consider $\kappa_{\rm pPb} = 2.1\ {\rm GeV\,fm^{-1}}$ at $\sqrt{s_{\rm NN}} = 5.02$ TeV, which fit charged particle production ($\mathrm{d}N_{\rm ch}/\mathrm{d}\eta$) [116, 117] at mid-pseudorapidity in minimum bias (MB) event selection of p + Pb interactions [65]. For $p + p$ collisions at $\sqrt{s} = 5.02$ TeV we use a constant cut-off parameter $p_{0_{\rm pp}} = 2\,{\rm GeV\,c^{-1}}$and an effective string tension value of $\kappa_{\rm pp} = 1.9\,{\rm GeV\,fm^{-1}}$.

The ALICE Collaboration at the LHC published first experimental data on the charged hadron multiplicity density at mid-rapidity in central (0–5%) Pb + Pb collisions at $\sqrt{s_{\rm NN}} = 2.76$ TeV [118, 119]. In this experiment the collaboration confirmed the presence of jet quenching ($R_{\rm AA} < 1$) [120, 121]. These results provide stringent constraints on the theoretical predictions in Pb + Pb collisions at LHC energies.

In order to describe new Pb + Pb data [118–121], we modified in HIJING/B$\bar{\rm B}$ v2.0 model (see ref. [62]) the main parameters describing hard partons interactions. For a parton a, the energy loss per unit distance can be expressed as $\mathrm{d}E_a/\mathrm{d}x = \epsilon_a/\lambda_a$, where $\epsilon_{\rm a}$ is the radiative energy loss per scattering and $\lambda_{\rm a}$ is the mean free path (mfp) of the inelastic scattering. For a *quark jet* at the top RHIC energy ($\sqrt{s_{\rm NN}} = 0.2$ TeV) $(\mathrm{d}E_q/\mathrm{d}x)_{\rm RHIC} = 1\,{\rm GeV\,fm^{-1}}$ and mfp $(\lambda_q)_{\rm RHIC} = 2$ fm [59]. The initial parton density is proportional to the final hadron multiplicity density. The charged particle density at mid-pseudorapidity at $\sqrt{s_{\rm NN}} = 2.76$ TeV is a factor of 2.2 higher than at $\sqrt{s_{\rm NN}} = 0.2$ TeV [118]. Therefore, for a *quark jet* at the LHC, the energy loss (mfp) should increase (decrease) by a factor of ≈2.0 and become $(\mathrm{d}E_q/\mathrm{d}x)_{\rm LHC} \approx 2\,{\rm GeV\,fm^{-1}}$ and mfp $(\lambda_q)_{\rm LHC} \approx 1$ fm. For a gluon jet $\mathrm{d}E_g/\mathrm{d}x = 2\ \mathrm{d}E_{\rm q}/\mathrm{d}x$.

Throughout this analysis we will consider the results with the following set of parameters for hard interactions: i.e., K=1.5; $\mathrm{d}E_q/\mathrm{d}x = 2\,\mathrm{GeV\,fm^{-1}}$; and $\lambda_q = 1\,\mathrm{fm}$. Since there is always a coronal region with an average length λ_q in the system where the produced parton jets will escape without scattering or energy loss, the suppression factor can never be infinitely small. For the same reason, the suppression factor should also depend on λ_q. It is difficult to extract information on both $\mathrm{d}E_q/\mathrm{d}x$ and λ_q simultaneously from the measured spectra in a model independent way [122].

In the next section we show that a constant radiative energy loss mechanism (dE/dx = const) and jet quenching mechanism as implemented in the HIJING/B$\bar{\mathrm{B}}$ v2.0 model provide a good description of the suppression at intermediate and high p_T ($4 < p_\mathrm{T} < 15\,\mathrm{GeV\,c^{-1}}$) of charged particles and prompt charmed mesons production in Pb + Pb collisions at LHC energies.

3. Numerical results and discussion

3.1. Prompt open charm production in p + p collisions

The ALICE Collaboration has reported measurements of the transverse momentum distribution of prompt open charmed mesons ($\mathrm{D^0}$, $\mathrm{D^+}$, $\mathrm{D^{*+}}$, $\mathrm{D_s^+}$) in $p + p$ collisions at $\sqrt{s}$ = 7 TeV [73, 74], and of ($\mathrm{D^0}$, $\mathrm{D^+}$, $\mathrm{D^{*+}}$) at $\sqrt{s}$ = 2.76 TeV [72] in the central rapidity range $|y| \leqslant 0.5$. *Prompt* indicates D mesons produced at the $p + p$ interaction point, either directly in the hadronization of the charm quark or in strong decay of excited charm resonances. The contribution from weak decays of beauty mesons, which give rise to feed-down D mesons, were subtracted. The model calculations include SCF effects as discussed in section 2.1. The energy dependence of string tension from equation (8), $\kappa(s) = \kappa_0\,(s/s_0)^{0.04}$ GeV fm^{-1}, predict a modest increase when going from $\sqrt{s}$ = 2.76 TeV (κ=1.88 GeV fm^{-1}) to $\sqrt{s}$ = 7 TeV (κ = 2.03 GeV fm^{-1}). Therefore, to calculate prompt open charmed mesons production we consider the same value of average string tension for charm and strange quark, i.e, $\kappa_c = \kappa_s \approx 2\,\mathrm{GeV\,fm^{-1}}$. The theoretical results are compared to data in figure 1.Predictions for $\mathrm{D_s^+}$ mesons at $\sqrt{s}$ = 2.76 TeV are also included. The agreement between theory and experiment is good within experimental uncertainties, except at $\sqrt{s}$ = 7 TeV where while the average cross-section is well reproduced the predicted spectrum has a somewhat shallower slope than the data.

The results at $\sqrt{s}$ = 7 TeV are also reasonably well described by FONLL calculations [22], NLO pQCD calculations [20], and GM-VFNS model at $p_\mathrm{T} > 3\,\mathrm{GeV\,c^{-1}}$ [84]. The limited statistics of the experimental data at $\sqrt{s}$ = 2.76 TeV [72] prevents the use of these measurements as a baseline for R_PbPb studies of prompt charmed hadrons. Instead in [16, 72] in calculating R_PbPb at $\sqrt{s_\mathrm{NN}}$ = 2.76 TeV the baseline $p + p$ spectrum was obtained by a pQCD-driven s-scaling of the $p + p$ differential cross-section from $\sqrt{s}$ = 7 TeV to $\sqrt{s}$ = 2.76 TeV [16, 22]. The scaled D meson cross-sections at 2.76 TeV were found to be consistent with those measured with only a limited precision of 20–25% [72]. In this paper we use as baseline for calculations of NMF R_PbPb at $\sqrt{s_\mathrm{NN}}$ = 2.76 TeV, $p + p$ theoretical results obtained with HIJING/B$\bar{\mathrm{B}}$ v2.0 model.

3.2. NMFs in Pb + Pb collisions at $\sqrt{s_\mathrm{NN}} = 2.76\,TeV$

The NMF R_PbPb has been measured by the ALICE Collaboration for the centrality classes 0–20% and 40–80% in Pb + Pb collisions at $\sqrt{s_\mathrm{NN}}$ = 2.76 TeV for prompt $\mathrm{D^0}$, $\mathrm{D^+}$ and $\mathrm{D^{*+}}$ [79]. The results of the HIJING/B$\bar{\mathrm{B}}$ v2.0 model for p_T spectra in $p + p$ (lower histogram) and

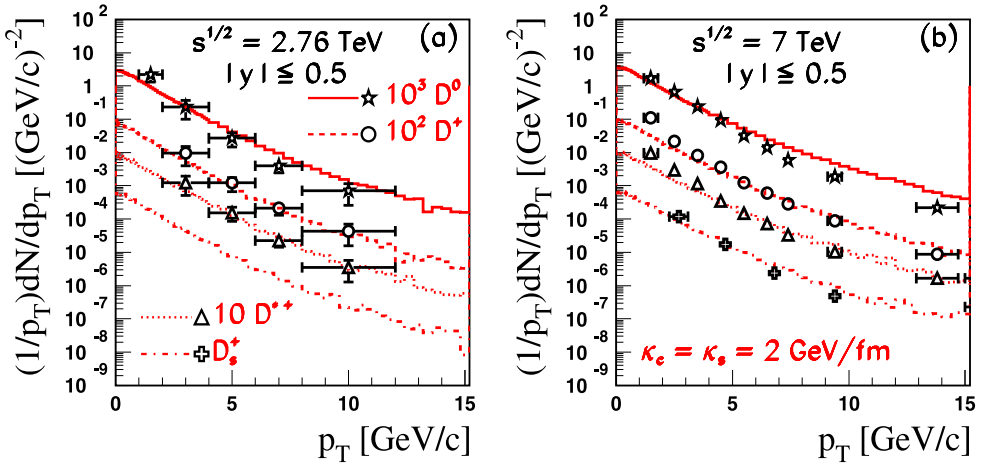

Figure 1. HIJING/B$\bar{\text{B}}$ v2.0 predictions for p_{T} distributions at mid-rapidity for $p + p \rightarrow (\text{D} + \bar{\text{D}})/2 + \text{X}$ with D = D^0 (solid histograms); D = D$^+$ (dashed histogram); D = D^{*+} (dotted histograms); and D = D$_s^+$ (dash-dotted histogram). The results are compared to data at $\sqrt{s}$ = 2.76 TeV (left panel) from [72] and at $\sqrt{s}$ = 7 TeV (right panel) from [73, 74]. For clarity, the experimental data and theoretical results are multiplied with a factor indicated in the figure. Only statistical error bars are shown.

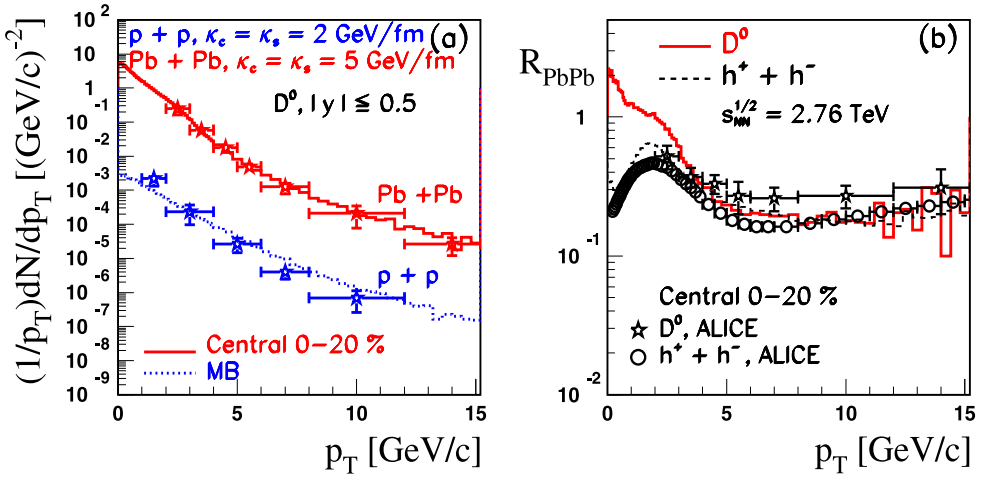

Figure 2. (a) HIJING/B$\bar{\text{B}}$ v2.0 predictions for p_{T} distributions at mid-rapidity for Pb + Pb $\rightarrow$ (D^0 + $\bar{\text{D}}^0$)/2 + X (upper histogram), and for $p + p$ collisions (lower histogram). (b) The p_{T} dependence of NMF $R_{\text{AA}}(p_{\text{T}})$ for D^0 mesons (solid histogram) and charged particles (dashed histogram) in central (0–20%) Pb + Pb collisions. Data are from ALICE Collaboration for D^0 (stars) [79] and for charged particles (open circles) [121]. Error bars include only statistical uncertainties.

central 0–20% Pb + Pb collisions (upper histogram) are compared to data [79] in figure 2 (left panel). For Pb + Pb collisions the results include quenching and shadowing effects as discussed in section 2.2 In the calculations we take into account the variation of strong color (electric) field with energy and the size of the colliding system. The assumed average string

tension is $\kappa_c = \kappa_s = 2.0\,\mathrm{GeV\,fm^{-1}}$ and $\kappa_c = \kappa_s = 5.0\,\mathrm{GeV\,fm^{-1}}$ for $p + p$ and Pb + Pb collisions, respectively. The agreement with the data is good except for $p + p$ reactions, where the slope of the predicted spectrum is, as it already mentioned in the section 3.1, a bit shallower than seen in the data.

The transverse momentum spectra of identified particles carrying light quarks and their azimuthal distributions are well described by hydrodynamical models [123, 124] at low p_T. The calculated spectra for D^0 mesons show a small shoulder at very low p_T indicating possible infuence of radial flow. However, since in the string model the pressure is not considered it is not expected to describe the sizable elliptic flow of heavy quarks observed by the ALICE Collaboration [79].

The transverse momentum dependence of the D^0 NMF $R^{D^0}_{PbPb}$ is shown in figure 2 (right panel). At transverse momentum $p_T > 6\,\mathrm{GeV\,c^{-1}}$ the charmed mesons show a suppression factor of ≈4. Also shown is a comparison with results for lighter quark species, specifically charged hadrons [121]. HIJING/B$\bar{\mathrm{B}}$ model calculations have shown [62] that the charged-pions R^{π}_{PbPb} coincides with that of charged hadrons above $p_T \approx 6\,\mathrm{GeV\,c^{-1}}$ and are lower by 25–30% in the p_T range 2–4 $\mathrm{GeV\,c^{-1}}$. At high $p_T > 6\,\mathrm{GeV\,c^{-1}}$ the calculated D^0 meson suppression is comparable with that of charged particles (and π mesons) within experimental uncertainties. This result indicates that the energy loss of charm quarks is rather similar to that of lighter quarks or gluons, in contrast with previous theoretical studies [31, 33].

At low p_T ($0 < p_T < 4\,\mathrm{GeV\,c^{-1}}$), the non-perturbative production mechanism via SCF produces a difference between D^0 and charged particles (mainly π mesons). The reason for this difference is that yields of charged particles are reduced due to conservation of energy [58] and yields of D mesons are enhanced due to an increase of $s\,\bar{s}$ and $c\,\bar{c}$ pair production (see equation (5)). In this range of p_T, the model predicts a quark-mass hierarchy, i.e., $R^{\pi}_{PbPb} < R^{ch}_{PbPb} < R^{D}_{PbPb}$. Within the model phenomenology we can interpret the above result as evidence for '*in-medium mass modification*' of charm quark due to possible chiral symmetry restoration [125]. An in-medium mass modification has also been predicted near the phase transition (i.e., at lower energy) in [126]. In contrast, the statistical hadronization model [127] predicts no medium effects at RHIC and LHC energies. Recent preliminary ALICE data [16, 81] suggest a decrease in going from low to high p_T albeit with big errors. Measurements with good statistics at low p_T are needed in order to draw a definite conclusion concerning the shape of the transverse momentum dependence of $R^{D}_{PbPb}(p_T)$. Similar results (not included here) are obtained for prompt D^+ and D^{*+} mesons.

When compared with figures 2 and 3 shows that the HIJING/B$\bar{\mathrm{B}}$ model predicts less suppression of D^0 mesons (solid histogram) from a factor ≈4 to ≈1.6 when going from from central 0–20% to semi-peripheral 40–80% Pb + Pb collisions. Once more, at high $p_T > 6\,\mathrm{GeV\,c^{-1}}$ the D^0 meson suppression is comparable within experimental uncertainties with that of charged particles (dashed histogram). These results are consistent with data for D^0 meson [79] and for charged particles [121]. At low p_T the split between D^0 mesons and charged particles is considerably reduced except at very low p_T ($p_T < 1\,\mathrm{GeV\,c^{-1}}$) where a modest quark-mass hierarchy $R^{ch}_{PbPb} < R^{D}_{PbPb}$ is predicted.

The suppression observed in NMF $R^{D^0}_{PbPb} < 1$ has contributions from initial and final states. Initial state effects (such as nuclear shadowing and gluon saturation) could be identified from the study of open charm production in p + Pb collisions. The initial production of $c\,\bar{c}$ pairs by gluon fusion might be suppressed due to gluon shadowing. We recall that shadowing is a depletion of the low-momentum parton distribution for a nucleon embedded in a nucleus as compared to a free nucleon. In the kinematic range of interest the nuclear shadowing will reduce the PDF for partons with nucleon momentum fraction x below 10^{-2}.

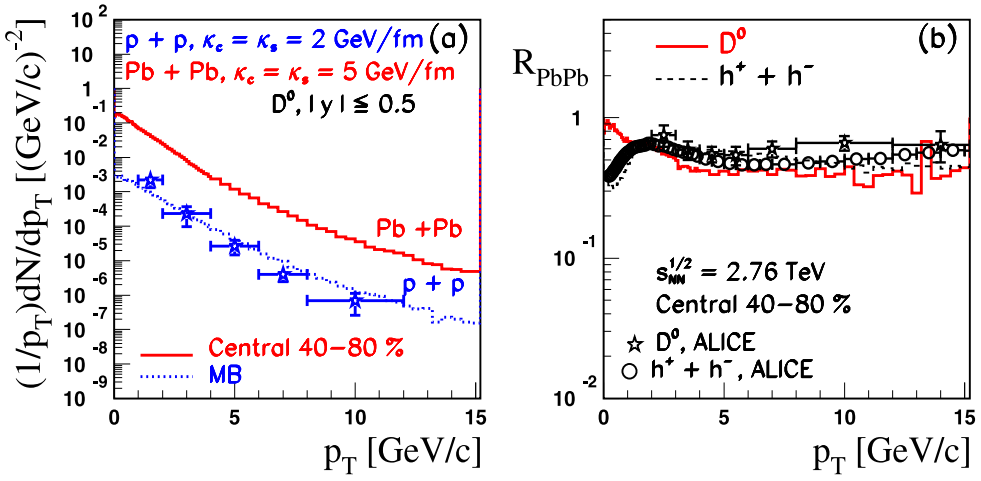

Figure 3. Comparison of HIJING/B$\bar{\text{B}}$ v2.0 predictions of p_{T} distributions (left panel) and NMF $R_{\text{AA}}(p_{\text{T}})$ for D^0 and charged particles in semi-peripheral (40–80%) Pb + Pb collisions (right panel). The histograms have the same meaning as in figure 2. Data are from the ALICE Collaboration for D^0 (stars) [79] and for charged particles (open circles) [121]. Error bars include only statistical uncertainties.

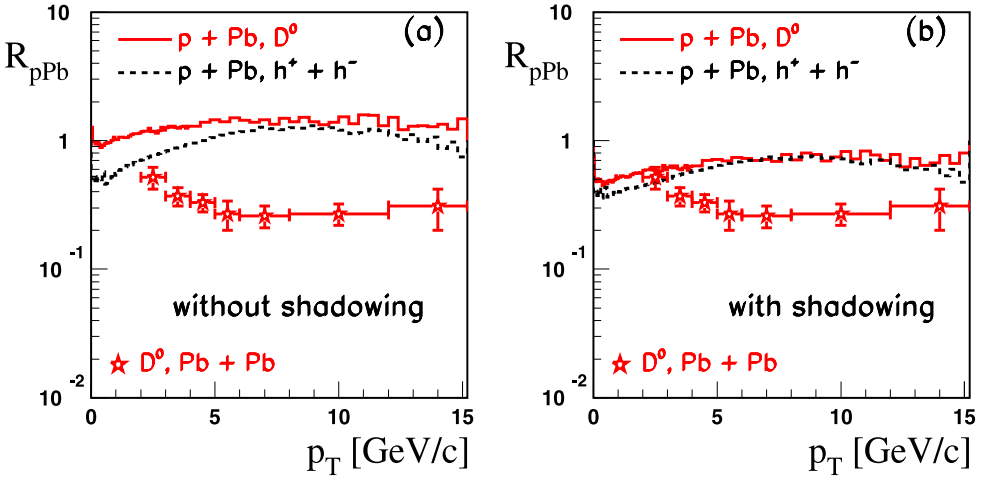

Figure 4. The HIJING/B$\bar{\text{B}}$ v2.0 model predictions for R_{pPb} of D^0 mesons (solid histograms) and charged particles (dashed histograms) in the 0–20% centrality class p + Pb colisions at $\sqrt{s_{\text{NN}}}$ = 5.02 TeV. The results assuming no shadowing (left panel) and with shadowing (right panel) are compared with experimental data on R_{PbPb} for D^0 mesons in the same centrality class (0–20%) at $\sqrt{s_{\text{NN}}}$ = 2.76 TeV. The data are from ref. [79]. Only statistical error bars are shown.

There is a considerable uncertainty (up to a factor of 3) in the amount of shadowing predicted at RHIC and LHC energies by the different models with HIJING predicting the strongest effect [128, 129]. The model predictions of $R_{\text{pPb}}^{\text{D}^0}$ in p + Pb collisions at $\sqrt{s_{\text{NN}}}$ = 5.02 TeV are presented in figure 4, for two scenarios, without (left panel) and with nuclear shadowing (right

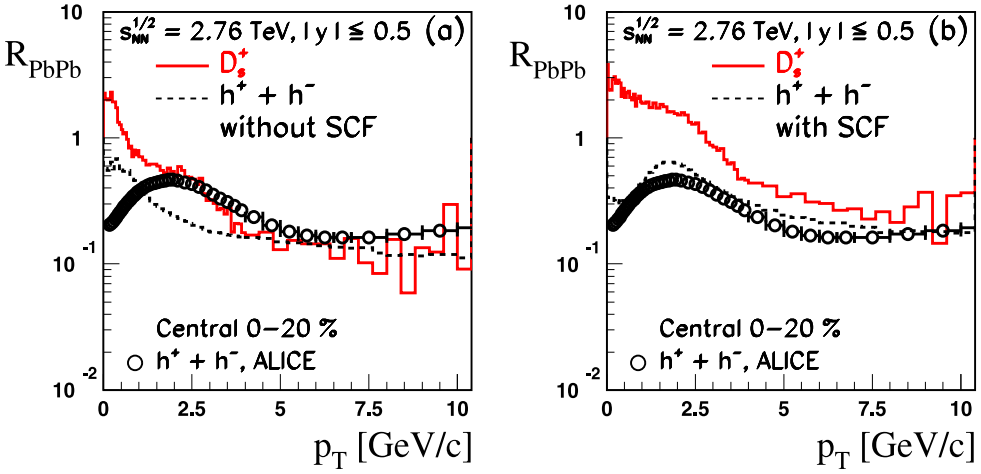

Figure 5. Comparison of HIJING/B$\bar{\text{B}}$ v2.0 predictions of nuclear modification factor $R_{PbPb}(p_T)$ for D_s^+ (solid histograms) and charged particles (dashed histograms) in central (0–20%) Pb + Pb collisions at mid-rapidity. The results are presented for a scenario without SCF effects (left panel) and with SCF effects (right panel) (see text for details). Data are from ALICE Collaboration [121]. Error bars include only statistical uncertainties.

panel), and compared to data obtained in the same centrality class at $\sqrt{s_{NN}}$ = 2.76 TeV [79]. We use shadowing parameterizations as discussed in section 2.2 Calculations without shadowing show no suppression except at low p_T where one observes some differences between D^0 and charged particles. Taking into account nuclear shadowing, the model predicts a suppression of ≈30% at high p_T for both charged particles (dashed histogram) and D^0 mesons (solid histogram). From this result, we may conclude that the strong suppression (a factor of ≈4) observed for $R_{PbPb}^{D^0}$ [79] is a final state effect (e.g., radiative and collisional energy loss in the QGP matter). Note that for MB measurements, R_{pPb}^{ch} is better described in a scenario without shadowing effects [63, 65]. Since we expect higher sensitivity to shadowing effects for D^0 mesons than for charged particles, measurements of R_{pPb}^{D} at LHC energies could help to resolve this puzzle.

Due to its strange quark content the study of the production of prompt charmed mesons D_s^+ ($c\,\bar{s}$) and D_s^- ($\bar{c}\,s$) is of particular interest. Our model predicts higher sensitivity to SCF effects for strange-charmed D_s^+ mesons than for the non-strange charmed mesons (D^0, D^+, D^{*+}). In figure 5, theoretical predictions for the p_T dependence of $R_{PbPb}^{D_s}$ for D_s^+ mesons (solid histograms) and R_{PbPb}^{ch} for charged particles (dashed histograms) are presented for two scenarios: without (left panel) and with (right panel) SCF effects. The calculations without SCF contributions assume for the string tension a vacuum value $\kappa_c = \kappa_s = \kappa_0 = 1$ GeV fm^{-1} while the results with SCF are obtained including the energy and mass dependent, $\kappa_c = \kappa_s \approx 5$ GeV fm^{-1} (see section 2.2). The calculations also include shadowing and quenching effects. The importance of in-medium string tension values $\kappa_c = \kappa_s = 5$ GeV fm^{-1} is supported by data. Only with SCF effects included, does the model describe well charged particle NMF. SCF induces a difference at low p_T ($0 < p_T < 4$ GeV c^{-1}) between strange-charmed mesons D_s^+ and charged particles via non-perturbative production mechanism. The yields of strange-charmed mesons D_s^+ are enhanced due to an increase of $c\bar{c}$ and $s\bar{s}$ pairs production (see

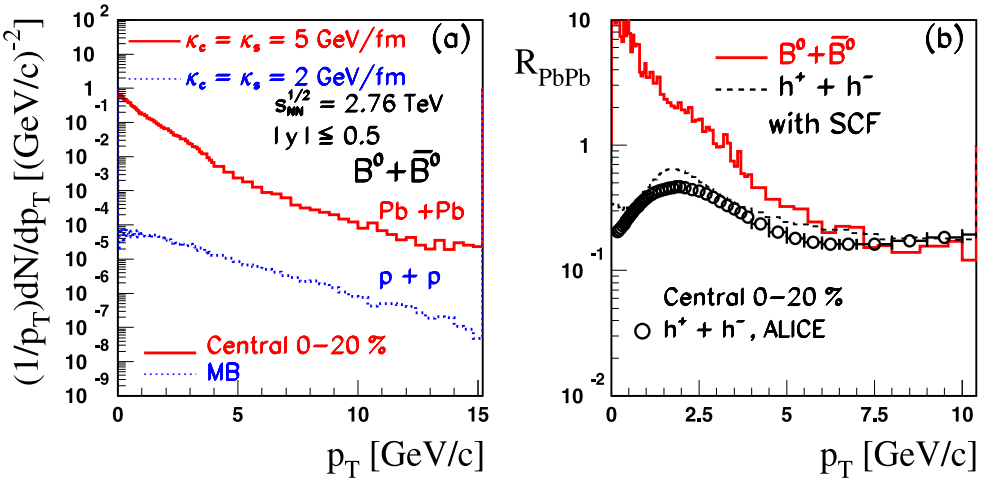

Figure 6. (a) HIJING/B$\bar{\text{B}}$ v2.0 predictions for p_{T} distributions at mid-rapidity for Pb + Pb (upper histogram), and for $p + p$ collisions (lower histogram) $\rightarrow (\text{B}^0 + \bar{\text{B}}^0)/2 + \text{X}$. (b) The p_{T} dependence of NMF $R_{\text{AA}}(p_{\text{T}})$ for B^0 mesons (solid histogram) and charged particles (dashed histogram) in central (0–20%) Pb + Pb collisions. Data for charged particles (open circles) [121] are from the ALICE Collaboration. Error bars include only statistical uncertainties.

equation (5)). In this range of p_{T} the model predicts a quark-mass hierarchy, i.e., $R^{\pi}_{\text{PbPb}} < R^{\text{ch}}_{\text{PbPb}} < R^{\text{D}_s}_{\text{PbPb}}$, similar with that seen for non-strange charmed mesons.

The first experimental results of $R^{\text{D}_s}_{\text{PbPb}}$ for D_s mesons in centrality class 0–7.5% Pb + Pb collisions at $\sqrt{s_{\text{NN}}}$ = 2.76 TeV [130] show at high p_{T} a suppression factor of ≈5 and is compatible within uncertainties with those obtained for non-strange D mesons. However, at lower and moderate transverse momenta $2.5 < p_{\text{T}} < 8\ \text{GeV c}^{-1}$ the measured NMF $R^{\text{D}_s}_{\text{PbPb}}$ [130] indicates values higher than the results shown in figure 5 (right panel). We studied if one can find a scenario that would give a larger enhancement of total yields for D_s mesons. We consider the effect of a further increase of the string tension for charm quark from $\kappa_{\text{c}} = 5$ GeV fm^{-1} to $\kappa_{\text{c}} = 10$ GeV fm^{-1}, keeping a constant $\kappa_{\text{s}} = 5$ GeV fm^{-1} for strange quark. This allows to test a possible flavour dependence of κ, as suggested in [45]. These calculations (not included here) result in only a modest increase of $R^{\text{D}_s}_{\text{PbPb}}$ by approximately 10–15%. For values of sting tension between 5 and 10 GeV fm^{-1} a saturation seems to set in, possibly as an effect of energy and momentum conservation constraints.

Due to large uncertainties in the data [130] we can not draw yet a firm conclusion on possible enhancement of strange-charmed mesons over non-strange one as predicted by our approach. Note that, at low and moderate p_{T} ($0 < p_{\text{T}} < 8\ \text{GeV c}^{-1}$) other complex dynamical mechanisms such as transport, diffusion, and coalescence could play an important role in a description of the $R^{\text{D}_s}_{\text{PbPb}}$ for D_s mesons at RHIC and LHC energies [131–133]. High statistics measurements in this p_{T} range could help to disentangle between different approaches.

In figures 6 and 7 we present predictions for beauty (b) quark production including results for non-strange B^0 and strange B^0_s mesons. For this calculations we used for the bottom mass $M_b^{\text{eff}} = 4.16$ GeV [94], and kept the same SCF parameters (i.e., $\kappa_b = \kappa_c = \kappa_s = 5$ GeV fm^{-1}). The results for the NMF display a bump in the p_{T} range 0.5–4 GeV c^{-1} with $R_{\text{AA}} > 1$ and a depletion at high p_{T}. Since the quark mass play a negligible role at very large p_{T}, the model predicts the same supression for charm, bottom and light quarks. On the other

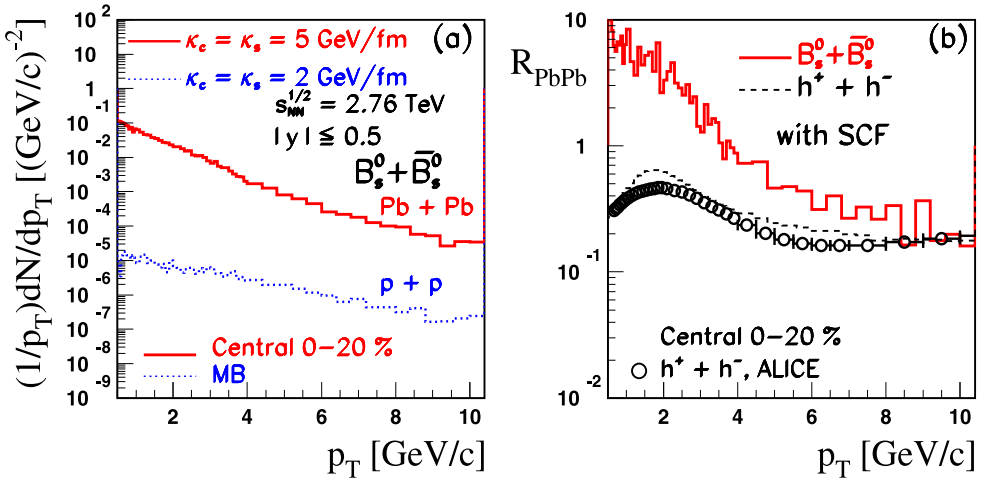

Figure 7. (a) HIJING/B$\bar{\text{B}}$ v2.0 predictions for p_{T} distributions at mid-rapidity for Pb + Pb (upper histogram), and for $p + p$ collisions (lower histogram) → $(\text{B}_s^0 + \bar{\text{B}}_s^0)/2$ + X . (b) The p_{T} dependence of NMF $R_{\text{AA}}(p_{\text{T}})$ for B_s^0 mesons (solid histogram) and charged particles (dashed histogram) in central (0–20%) Pb + Pb collisions. Data for charged particles (open circles) [121] are from the ALICE Collaboration. Error bars include only statistical uncertainties.

hand, at small and moderate p_{T}, the bump mainly due to SCF effects is modified in amplitude and increases with increasing quark mass. Such a non-trivial behaviour at low p_{T} if confirmed by experimental data, could be a crucial test for the role of SCF effects on heavy quark production at the LHC.

The NMF for strange mesons B_s^0 (figure 7) is enhanced by ≈20–30% in comparison with that for non-strange mesons B^0 (figure 6) due to an increase of $b\bar{b}$ and $s\bar{s}$ pairs production in Pb + Pb collisions (see equation (5)). In the moderate range of transverse momentum the model predicts a quark-mass hierarchy, i.e., $R_{\text{PbPb}}^{\pi} < R_{\text{PbPb}}^{\text{ch}} < R_{\text{PbPb}}^{\text{B}^0} < R_{\text{PbPb}}^{\text{B}_s^0}$, similar to that observed for charmed mesons.

3.3. D meson ratios

The inclusive p_{T} distributions for prompt open charm mesons (D^0, D^+, D^{*+}, D_s^+) in $p + p$ collisions at $\sqrt{s}$ = 7 TeV were shown in figure 1. As noted in the caption of figure 1 the reported yields refer to particles only, being computed as the average of particles and anti-particles, in order to improve statistical uncertainties. This assume that the production cross-section is the same for particle (D) and antiparticle ($\bar{\text{D}}$). The HIJING/B$\bar{\text{B}}$ v2.0 model predictions for the p_{T} dependence of ratios of non-strange mesons D^+ and D^{*+} to D^0 are shown in figure 8. To allow comparison with data only D mesons in the rapidity range $|y| < 0.5$ were considered.

The D^+/D^0 and D^{*+}/D^0 ratios are determined in the model by an input parameter $P_{\text{V}} = V/(V + S)$, that defines the fraction of D mesons in vector state (V) to all produced mesons (vectors (V) + scalars (S)). The solid histograms in figure 8 are obtained with the default value based on spin counting stattistics (i.e., $P_{\text{V}} = 3/(3 + 1) = 0.75$). Taking rather for P_{V} a value from the measured fractions of heavy flavour mesons produced in a vector state $P_V^{\text{exp.}} = 0.54$ [74], results in an enhancement of the D^+/D^0 ratio (left panel) and a reduction of

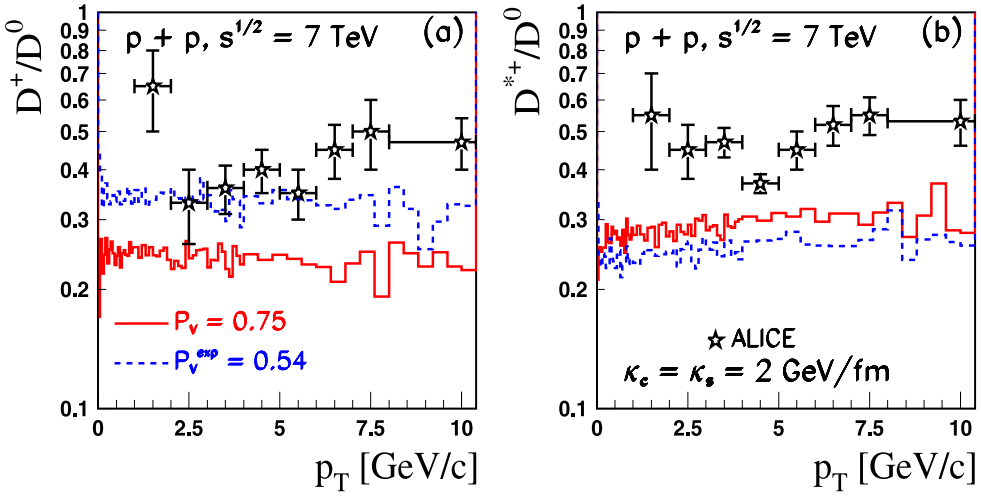

Figure 8. Comparison of HIJING/B$\bar{\text{B}}$ v2.0 predictions for ratios of non-strange D mesons; D^+/D^0 (left panel) and D^{*+}/D^0 (right panel). Two sets of results are shown, corresponding to default fraction P_V = 0.75 solid histograms and for the measured fraction P_V^{exp} = 0.54 dashed histograms (see text for explanation). The data are from refs. [73, 74]. Error bars include only the statistical uncertainty.

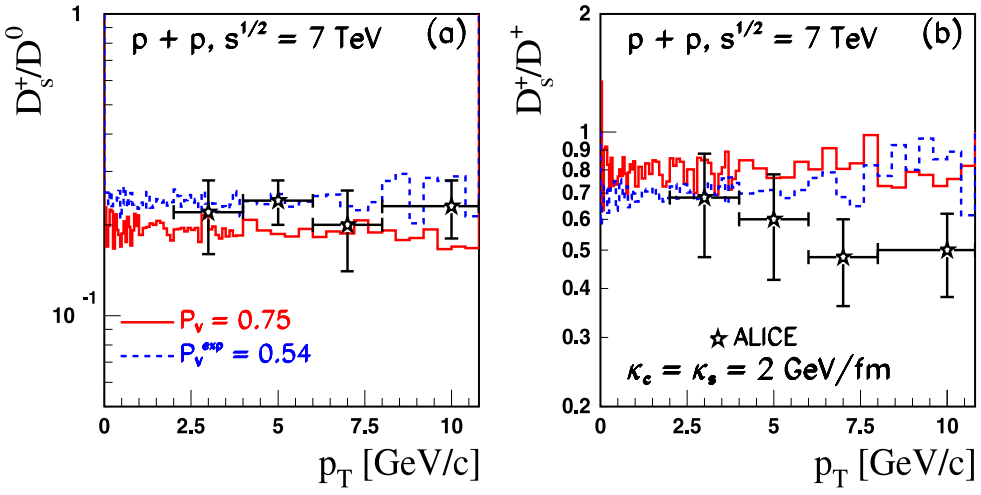

Figure 9. Comparison of HIJING/B$\bar{\text{B}}$ v2.0 predictions for ratios of strange $D_s^+$to non-strange mesons D^0 (left panel) and D^+ (right panel). The histograms have the same meaning as in figure 8. The data are from refs. [73, 74]. Error bars include only the statistical uncertainty.

D^{*+}/D^0 ratio (right panel) as compared to those obtained with the P_V default value. The agreement with data is improved for the D^+/D^0 ratio. On the other hand, the D^{*+}/D^0 ratio is underestimated by a factor of ≈1.5, since the model predicts a smaller cross sections for resonance production of D^{*+} mesons.

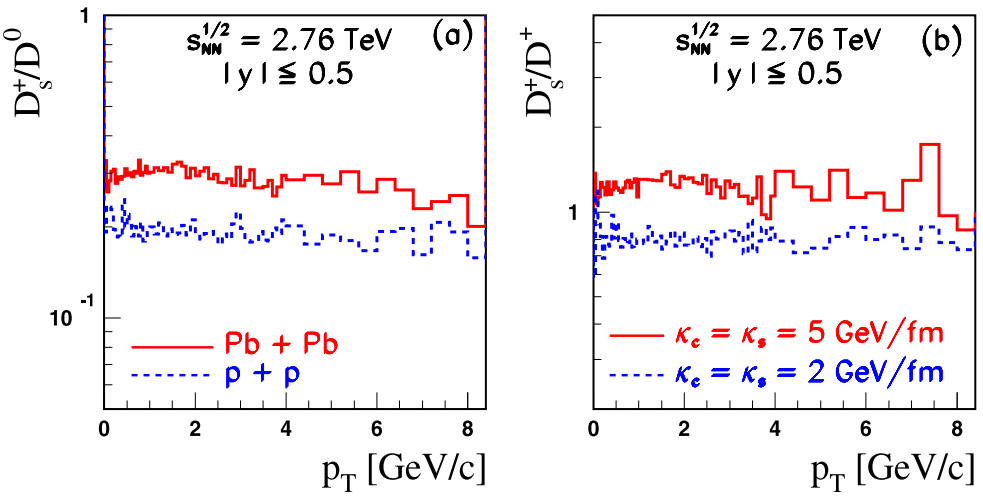

Figure 10. Comparison of HIJING/B$\bar{\text{B}}$ v2.0 predictions for ratios of strange $D_s^+$to non-strange mesons D^0 (left panel) and D^+ (right panel) at $\sqrt{s}$ = 2.76 TeV in $p + p$ collisions and at $\sqrt{s_{\rm NN}}$ = 2.76 TeV in centrality class 0–20% in Pb+Pb collisions. The results are shown for $\kappa_c = \kappa_s = 2$ GeV fm^{-1} (dashed histogram) and for in medium value $\kappa_c = \kappa_s = 5$ GeV fm^{-1} (solid histograms). The parameter $P_{\rm V}$ is set at its default value $P_{\rm V} = 0.75$.

The ratios of prompt strange D_s^+ mesons to the non-strange D^0 mesons and D^+ are plotted in figure 9. These ratios are mainly controlled by another input parameter $\gamma_{\rm s}$, that defines the s/u quark suppression factor in the fragmentation process. In the HIJING/B$\bar{\text{B}}$ v2.0 model this parameter is set to $\gamma_{\rm s} = 0.45$ using an energy dependent κ in $p + p$ collisions, and leads to an enhanced production of D_s^+ mesons, when compared with that using the default value $\gamma_{\rm s} = 0.3$. Note that $\gamma_{\rm s} = 0.45$ is compatible within total uncertainties with the measured value [74], $\gamma_s^{\rm exp}$= 0.31 $\pm$ 0.08(stat) $\pm$ 0.10(sys) $\pm$ 0.02(BR); here BR stands for decay branching ratios.

The calculations describe fairly well the D_s^+/D^0 ratio, while slightly overestimating the D_s^+/D^+ ratio. These ratios show almost no $p_{\rm T}$ dependence due to a very small difference between the fragmentation function of charm quarks to strange and non-strange mesons. Note that PYTHIA with Perugia-0 tune (using $\gamma_s = 0.2$) underestimates the prompt strange meson production [74]. More precise data are clearly needed to reach a firmer conclusion.

It will be interesting to study whether the ratios of strange to non-strange charmed mesons, i.e., D_s^+/D^0 and D_s^+/D^+ are enhanced in central Pb + Pb collisions relative to $p + p$ collisions. In figure 10 are shown the calculated ratios obtained at the same c. m. energy. The calculations are performed using $\kappa_c = \kappa_s = 2$ GeV fm^{-1} in $p + p$ collisions (dashed histograms) and with in-medium value $\kappa_c = \kappa_s = 5$ GeV fm^{-1} (solid histograms) in the case of Pb + Pb collisions. An enhancement of a factor of ≈2 is predicted by the HIJING/B$\bar{\text{B}}$ v2.0 model in going from $p + p$ MB events to central Pb + Pb collisions. Measurements in this region will be critical for testing the validity of models.

4. Summary and conclusions

In summary, we studied the influence of possible strong homogeneous constant color electric fields on prompt open charm mesons (D^0, D^+, D^{*+}, D_s^+) production in Pb + Pb and MB p + p

collisions in the framework of the HIJING/BB̄ v2.0 model. The measured ratios of prompt strange D_s^+ mesons to the non-strange D^0 and D^+ mesons in MB $p + p$ collisions at $\sqrt{s} = 7$ TeV help to verify our assumptions and to set the strangeness suppression factor for charm mesons. We assume an energy and system dependence of the effective string tension, κ, equivalent to an *in-medium mass* modification of charm and strange quark. The effective string tension control $Q\bar{Q}$ pair creation rates and suppression factors $\gamma_{Q\bar{Q}}$.

For Pb + Pb collisions at $\sqrt{s_{NN}} = 2.76$ TeV all nuclear effects included in the model, e.g., strong color fields, shadowing and quenching should be taken into account. Partonic energy loss and jet quenching process as embedded in the model achieve a reasonable description of the suppression ($R^D_{PbPb} < 1$) at moderate and high transverse momentum. Moreover, at low and intermediate p_T ($0 < p_T < 8$ GeV c^{-1}) the model predicts a quark mass hierarchy as suggested in ref. [32]. By computing the NMF R^D_{PbPb}, we show that the above nuclear effects constitute important dynamical mechanisms that explain better the observed prompt D mesons and charged particles production as observed by the ALICE collaboration.

The initial production of $c\ \bar{c}$ pairs by gluon fusion might be suppressed due to initial state effects (e.g. gluon shadowing or saturation). By computing the NMF R^D_{pPb} in central$p$ + Pb collisions at $\sqrt{s_{NN}} = 5.02$ TeV including shadowing effects, we conclude that the strong suppression observed for R^D_{PbPb} is due to a final state effect. Measurements with high statistics at low p_T ($0 < p_T < 4$GeV c^{-1}) of the NMF R^D_{PbPb} and R^B_{PbPb} in Pb + Pb central collisions could help to disentangle between different model approaches and/or different dynamical mechanisms, especially for D_s^+ ($c\bar{s}$) and B_s^0 ($b\bar{s}$) mesons, due to their quark content.

The HIJING/BB̄ model is based on a time-independent color field strength while in reality the production of $Q\bar{Q}$ pairs is more complex being a far-from-equilibrium, time and space dependent phenomenon. To achieve more quantitative conclusions, such time and space dependent mechanisms [45, 69] should be considered in future generations of Monte Carlo codes.

Acknowledgments

This work is supported by the Natural Sciences and Engineering Research Council of Canada (V Topor Pop, J Barrette, and C Gale), by the Division of Nuclear Science, US Department of Energy, under Contract No. DE-AC03-76SF00098 and DE-FG02-93ER-40764 (associated with the JET Topical Collaboration Project, M Gyulassy), and by the Romanian Authority for Scientific Research, CNCS-UEFISCDI project number PN-II-ID-2011-3-0368 (M Petrovici, and V Topor Pop partial support).

References

[1] Hwa R C and Wang X N (ed) 2010 *Quark Gluon Plasma* 4 (Singapore: World Scientific)
[2] Muller B, Schukraft J and Wyslouch B 2012 *Annu. Rev. Nucl. Part. Sci.* **62** 361
[3] Jacak B V and Muller B 2012 *Science* **337** 310
[4] Bazavov *et al* 2012 *Phys. Rev.* D **85** 054503
[5] Muller B and Wang X N 1992 *Phys. Rev. Lett.* **68** 2437
[6] Shuryak E V 1992 *Phys. Rev. Lett.* **68** 3270
[7] Geiger K 1993 *Phys. Rev.* D **48** 4129
[8] Kuznetsova I and Rafelski J 2006 *J. Phys. G: Nucl. Part. Phys.* **32** S499
[9] He M, Fries R J and Rapp R 2012 *Phys. Rev.* C **86** 014903
[10] Frawley A D, Ullrich T and Vogt R 2008 *Phys. Rep.* **462** 125
[11] Gale C and Ruan L 2013 *Nucl. Phys.* A **904–905** 334c

[12] Mischke A 2013 *Proc. 10th Quark Confinement and the Hadron Spectrum (TUM Campus Garching, Munich, Germany, 8–12 October 2012)* arXiv:1301.7550 [hep-ex]
[13] Andronic A *et al* (ALICE Collaboration) 2013 *J. Phys.: Conf. Ser.* **455** 012002
[14] Dainese A 2011 *J. Phys. G: Nucl. Part. Phys.* **38** 124032
[15] Dainese A (ALICE Collaboration) 2013 *Presented at 23rd Int. Conf. in High Energy Physics (ICHEP 2012) (Melbourne, Australia, 4–11 July 2012)* PoS ICHEP2012 417
[16] del Valle Z C (ALICE Collaboration) 2013 *Nucl. Phys.* A **904-905** 178c
[17] Zhu X, Bleicher M, Huang S, Schweda K L, Stoecker H, Xu N and Zhuang P 2007 *Phys. Lett.* B **647** 366
[18] Linnyk O, Bratkovskaya E L and Cassing W 2008 *Int. J. Mod. Phys.* E **17** 1367
[19] Lin Z W and Gyulassy M 1995 *Phys. Rev.* C **51** 2177
Lin Z W and Gyulassy M 1995 *Phys. Rev.* C **52** 440 (erratum)
[20] Mangano M L, Nason L P and Ridolfi G 1992 *Nucl. Phys.* B **373** 295
[21] Vogt R 2008 *Eur. Phys. J. Spec. Top.* **155** 213
Cacciari M, Nason M P and Vogt R 2005 *Phys. Rev. Lett.* **95** 122001
[22] Cacciari M, Frixione M S, Houdeau N, Mangano M L, Nason P and Ridolfi G 2012 *J. High Energy Phys.* JHEP10(2012)137
[23] Abelev B I *et al* (STAR Collaboration) 2007 *Phys. Rev. Lett.* **98** 192301
Abelev B I *et al* (STAR Collaboration) 2011 *Phys. Rev. Lett.* **106** 159902 (erratum)
[24] Zhang Y F 2008 *J. Phys. G: Nucl. Part. Phys.* **35** 104022
[25] Adler S S *et al* (PHENIX Collaboration) 2006 *Phys. Rev. Lett.* **96** 032301
[26] Adare A *et al* (PHENIX Collaboration) 2007 *Phys. Rev. Lett.* **98** 172301
[27] Uphoff J, Fochler O, Xu Z and Greiner C 2010 *Phys. Rev.* C **82** 044906
[28] Tannenbaum M J 2013 *Proc. 50th Int. School of Subnuclear Physics: What we would like LHC to give us* (*ISSP 2012*) (*Erice, Italy, 23 June–2 July 2012*) pp 347–67 arXiv:1302.1833 [nucl-ex]
[29] Gyulassy M and Plumer M 1990 *Phys. Lett.* B **243** 432
[30] Baier R, Schiff D and Zakharov B G 2000 *Annu. Rev. Nucl. Part. Sci.* **50** 37
[31] Dokshitzer Y L and Kharzeev D E 2001 *Phys. Lett.* B **519** 199
[32] Armesto N, Dainese A, Salgado C A and Wiedemann U A 2005 *Phys. Rev.* D **71** 054027
[33] Wicks S, Horowitz W, Djordjevic M and Gyulassy M 2007 *Nucl. Phys.* A **783** 493
[34] Zichichi A 2008 *Nucl. Phys.* A **805** 36
[35] Schwinger J S 1951 *Phys. Rev.* **82** 664
[36] Biro T S, Nielsen H B and Knoll J 1984 *Nucl. Phys.* **B245** 449
[37] Gyulassy M and Iwazaki A 1985 *Phys. Lett.* B **165** 157
[38] Tanji N 2009 *Ann. Phys.* **324** 1691
[39] Ruffini R, Vereshchagin G and Xue S S 2010 *Phys. Rep.* **487** 1
[40] Labun L and Rafelski J 2009 *Phys. Rev.* D **79** 057901
[41] Cardoso N, Cardoso M and Bicudo P 2012 *Phys. Lett.* B **710** 343
[42] Nayak G C 2005 *Phys. Rev.* D **72** 125010
[43] Nayak G C and Nieuwenhuizen P 2005 *Phys. Rev.* D **71** 125001
[44] Levai P and Skokov V V 2009 *J. Phys. G: Nucl. Part. Phys.* **36** 064068
[45] Levai P and Skokov V V 2010 *Phys. Rev.* D **82** 074014
[46] Levai P and Skokov V V 2011 *AIP Conf. Proc.* **1348** 118
[47] Levai P, Berenyi D, Pasztor A and Skokov V V 2011 *J. Phys. G: Nucl. Part. Phys.* **38** 124155
[48] Andersson B, Gustafson G, Ingelman G and Sjostrand T 1983 *Phys. Rep.* **97** 31
[49] Wang X N and Gyulassy M 1992 *Phys. Rev. Lett.* **68** 1480
Wang X N and Gyulassy M 1991 *Phys. Rev.* D **44** 3501
[50] Casher A, Neuberger A H and Nussinov A 1979 *Phys. Rev.* D **20** 179
Casher A, Neuberger A H and Nussinov A 1980 *Phys. Rev.* D **21** 1966
[51] Gelis F, Lappi T and McLerran L 2009 *Nucl. Phys.* A **828** 149
Lappi T and McLerran L 2006 *Nucl. Phys.* A **772** 200
[52] McLerran L 2008 *J. Phys. G: Nucl. Part. Phys.* **35** 104001
[53] Kharzeev D, Levin E and Tuchin K 2007 *Phys. Rev.* C **75** 044903
[54] Braun M A, Pajares C and Vechernin V V 2013 *Nucl. Phys.* A **906** 14
[55] Deng W T, Wang X N and Xu R 2011 *Phys. Rev.* C **83** 014915
[56] Deng W T, Wang X N and Xu R 2011 *Phys. Lett.* B **701** 133
[57] Topor Pop V, Gyulassy M, Barrette J, Gale C, Wang X N and Xu N 2004 *Phys. Rev.* C **70** 064906

[58] Topor Pop V, Gyulassy M, Barrette J, Gale C, Bellwied R and Xu N 2005 *Phys. Rev.* C **72** 054901
[59] Topor Pop V, Gyulassy M, Barrette J, Gale C, Jeon S and Bellwied R 2007 *Phys. Rev.* C **75** 014904
[60] Topor Pop V, Barette J and Gyulassy M 2009 *Phys. Rev. Lett.* **102** 232302
[61] Topor Pop V, Gyulassy M, Barrette J, Gale C and Warburton A 2011 *Phys. Rev.* C **83** 024902
[62] Topor Pop V, Gyulassy M, Barrette J and Gale C 2011 *Phys. Rev.* C **84** 044909
[63] Barnafoldi G G, Barrette J, Gyulassy M, Levai P and Topor Pop V 2012 *Phys. Rev.* C **85** 024903
[64] Topor Pop V, Gyulassy M, Barrette J, Gale C and Warburton A 2012 *Phys. Rev.* C **86** 044902
[65] Albacete J L *et al* 2013 *Int. J. Mod. Phys.* E **22** 1330007
[66] Ripka G (ed) 2004 *Lecture Notes in Physics* vol 639 (Berlin: Springer) p 138
[67] Magas V K, Csernai L P and Strottman D 2002 *Nucl. Phys.* A **712** 167
[68] Cohen T D and McGady D A 2008 *Phys. Rev.* D **78** 036008
[69] Hebenstreit F, Alkofer R and Gies H 2008 *Phys. Rev.* D **78** 061701
[70] Merino C, Pajares C, Ryzhinskiy M M, Shabelski Y M and Shuvaev A G 2010 *Phys. At. Nucl.* **73** 1781
Merino C, Pajares C, Ryzhinskiy M M, Shabelski Y M and Shuvaev A G 2011 *Phys. At. Nucl* **74** 173 (erratum)
[71] Bautista I and Pajares C 2010 *Phys. Rev.* C **82** 034912
[72] Abelev B *et al* (ALICE Collaboration) 2012 *J. High Energy Phys.* JHEP07(2012)191
[73] Abelev B *et al* (ALICE Collaboration) 2012 *J. High Energy Phys.* JHEP01(2012)128
[74] Abelev B *et al* (ALICE Collaboration) 2012 *Phys. Lett.* B **718** 279
[75] ATLAS Collaboration 2011 *Report* No. ATLAS-CONF-2011-017
[76] Rossi E(ATLAS Collaboration) 2011 *Nuovo Cimento* C **034N06** 226
[77] ATLAS Collaboration 2012 *Report* No. ATLAS-CONF-2012-050.
[78] RAaij *et al* (HCb Collaboration) 2013 *Nucl. Phys.* B **871** 1
[79] Abelev B *et al* (ALICE Collaboration) 2012 *J. High Energy Phys.* JHEP09(2012)112
[80] Bailhache R(ALICE Collaboration) 2012 *J. Phys. Conf. Ser.* **389** 012023
[81] Grelli A (ALICE Collaboration) 2013 *Nucl. Phys.* A **904-905** 635c
[82] Valencia Palomo L L (ALICE Collaboration) 2012 *PoS QNP* **2012** 156
[83] Maciula R and Szczurek A 2013 *Phys. Rev.* D **87** 094022
[84] Kniehl B A, Kramer G, Schienbein I and Spiesberger H 2012 *Eur. Phys. J.* C **72** 2082
[85] Sharma R, Vitev I and Zhang B W 2009 *Phys. Rev.* C **80** 054902
[86] He Y, Vitev I and Zhang B W 2012 *Phys. Lett.* B **713** 224
[87] Horowitz W A and Gyulassy M 2011 *J. Phys. G: Nucl. Part. Phys.* **38** 124114
[88] Horowitz W A 2012 *AIP Conf. Proc.* **1441** 889
[89] Alberico W M *et al* 2011 *Eur. Phys. J.* C **71** 1666
[90] Monteno M *et al* 2011 *J. Phys. G: Nucl. Part. Phys.* **38** 124144
[91] Gossiaux P B, Bierkandt R and Aichelin J 2009 *Phys. Rev.* C **79** 044906
[92] Gossiaux P B, Aichelin J, Gousset T and Guiho V 2010 *J. Phys. G: Nucl. Part. Phys.* **37** 094019
[93] Buzzatti A and Gyulassy M 2012 *Phys. Rev. Lett.* **108** 022301
[94] Steinhauser M 2008 Continous advances in QCD *Proc. 8th Workshop, CAQCD-08, (Minneapolis, MN, 15–18 May 2008)* ed M Peloso (Hackensack, NJ: World Scientific) pp 90–7 arXiv:0809.1925 [hep-ph]
[95] Altarelli G and Parisi G 1977 *Nucl. Phys.* **B126** 298
[96] Cristoforetti M, Faccioli M P, Ripka G and Traini M 2005 *Phys. Rev.* D **71** 114010
[97] Nakamura K *et al* (Particle Data Group) 2010 *J. Phys. G: Nucl. Part. Phys.* **37** 075021
[98] Amelin N S, Armesto N, Pajares C and Sousa D 2001 *Eur. Phys. J.* C **22** 149
[99] Gribov L V, Levin E M and Ryskin M G 1983 *Phys. Rep.* **100** 1
[100] McLerran L and Praszalowicz M 2010 *Acta Phys. Polon.* B **41** 1917
[101] Dumitru A, Gelis F, McLerran L and Venugopalan R 2008 *Nucl. Phys.* A **810** 91
[102] Dusling K, Gelis F, Lappi T and Venugopalan R 2010 *Nucl. Phys.* A **836** 159
[103] Aamodt K *et al* (ALICE Collaboration) 2010 *Phys. Rev. Lett.* **105** 252301
[104] Abelev B *et al* (ALICE Collaboration) 2013 *Phys. Rev. Lett.* **110** 032301
[105] Andersson B, Gustafson G and Nilsson-Almqvist B 1987 *Nucl. Phys.* **B281** 289
Nilsson-Almqvist B and Stenlund E 1987 *Comput. Phys. Commun.* **43** 387
[106] Bengtsson H U and Sjostrand T 1987 *Comput. Phys. Commun.* **46** 43
[107] Sjostrand T, Mrenna S and Skands P Z 2006 *J. High Energy Phys.* JHEP05(2006)026

[108] Eichten E, Hinchliffe I, Lane K D and Quigg C 1984 *Rev. Mod. Phys.* **56** 579
Eichten E, Hinchliffe I, Lane K D and Quigg C 1986 *Rev. Mod. Phys.* **58** 1065 (addendum)
[109] Eskola K J and Wang X N 1995 *Int. J. Mod. Phys.* **A10** 3071
[110] Campbell J M, Huston J W and Stirling W J 2007 *Rep. Prog. Phys.* **70** 89
[111] Wang X N and Gyulassy M 1992 *Phys. Rev.* D **45** 844
[112] Duke D W and Owens J F 1984 *Phys. Rev.* D **30** 49
[113] Eskola K J 2002 *Nucl. Phys.* A **698** 78
[114] Eskola K J, Kajantie K, Ruuskanen P V and Tuominen K 2000 *Nucl. Phys.* **B570** 379
[115] Eskola K J, Kajantie K and Tuominen K 2001 *Phys. Lett.* **B497** 39
[116] Abelev B *et al* (ALICE Collaboration) 2013 *Phys. Rev. Lett.* **110** 032301
[117] Abelev B *et al* (ALICE Collaboration) 2013 *Phys. Rev. Lett.* **110** 082302
[118] Aamodt K *et al* (ALICE Collaboration) 2010 *Phys. Rev. Lett.* **105** 252301
[119] Aamodt K *et al* (ALICE Collaboration) 2011 *Phys. Rev. Lett.* **106** 032301
[120] Aamodt K *et al* (ALICE Collaboration) 2011 *Phys. Lett.* **B696** 30
[121] Abelev B *et al* (ALICE Collaboration) 2013 *Phys. Lett.* B **720** 52
[122] Wang X N 1998 *Phys. Rev.* C **58** 2321
[123] Heinz U W and Snellings R 2013 *Annu. Rev. Nucl. Part. Sci.* **63** 123
[124] Gale C, Jeon S and Schenke B 2013 *Int. J. Mod. Phys.* A **28** 1340011
[125] Kharzeev D and Tuchin K 2005 *Nucl. Phys.* A **753** 316
[126] Tolos L, Schaffner-Bielich J and Stoecker H 2006 *Phys. Lett.* B **635** 85
[127] Andronic A, Braun-Munzinger P, Redlich P K and Stachel J 2008 *J. Phys. G: Nucl. Part. Phys.* **35** 104155
[128] Li S Y and Wang X N 2002 *Phys. Lett.* **B527** 85
[129] d'Enterria D (CMS Collaboration) 2008 *J. Phys. G: Nucl. Part. Phys.* **35** 104039
[130] Innocenti G M 2013 *Nucl. Phys.* A **904-905** 433c
[131] He M, Fries R J and Rapp R 2013 *Phys. Rev. Lett.* **110** 112301
[132] Alberico W M, Beraudo A, De Pace A, Molinari A, Monteno M, Nardi M M, Prino F and Sitta M 2013 *Eur. Phys. J.* C **73** 2481
[133] Cao S, Qin G Y and Bass S A 2013 *Phys. Rev.* C **88** 044907